JOURNAL OF ENVIRONMENTAL HYDROLOGY

Open Access Online Journal of the International Association for Environmental Hydrology

VOLUME 24 2016

ASSESSMENT OF CLIMATE CHANGE IMPACTS ON WATER RESOURCES OF KHABOUR IN KURDISTAN, IRAQ USING SWAT MODEL

Nahlah Abbas[a]
Saleh A Wasimi[a]
Nadhir Al-Ansari[b]

[a]**School of Engineering & Technology**
Central Queensland University, Melbourne, Australia
[b]**Geotechnical Engineering**
Lulea University of Technology, Lulea, Sweden

The Khabour River is one of five tributaries of Tigris River and the first river flows into Tigris River contributing to Tigris Flow by about 2 BCM at Zakho Station. The area of this catchment is 6,143 km^2, of which 57% are located in Turkey and 43% in Iraq with a total length of 181 km. Khabour River is the main source of fresh water to Duhok City, one of the major cities of Kurdistan Region. Hydro-meteorological data over the past several decades reveal that the catchment is experiencing increasing variability in precipitation and stream flow contributing to more severe droughts and floods presumably due to climate change. SWAT model was applied to capture the dynamics of the basin. The model was calibrated at Zakho station. The performance of the model was rather satisfactory; R^2 and ENC were 0.5 and 0.51, respectively in calibration period. In validation process R^2 and ENC were nearly consistent. In the next stage, six GCMs from CMIP3 namely, CGCM3.1/T47, CNRM-CM3, GFDL-CM2.1, IPSLCM4, MIROC3.2 (medres) and MRI CGCM2.3.2 were selected for climate change projections in the basin under a very high emissions scenario (A2), a medium emissions scenario (A1B) and a low emissions scenario (B1) for two future periods (2046-2064) and (2080-2100). All GCMs showed consistent increases in temperature and decreases in precipitation, and as expected, highest rate for A2 and lowest rate for B1. The projected temperatures and precipitation were input to the SWAT model to project water resources, and the model outputs were compared with the baseline period (1980-2010), the picture that emerged depicted deteriorating water resources variability.

INTRODUCTION

Climate change is one of the major concerns confronting Iraq affecting all sectors of life especially water sector. Iraq is highly vulnerable to climate change due to its aridity. The impacts of climate change on water resources could deleteriously affect the environment and the socio-economy of the country, particularly the agricultural sector. There is a strong demand from decision makers for predictions about the potential impacts of climate change involving the duration and magnitude of precipitation, which has ramifications on sustaining and managing water resources appropriately to meet water scarcity that has become pronounced (Al-Ansari et al. 2014). Khabour tributary is one of Tigris Tributaries and the major water resource for Duhok City, one of the major cities of Kurdistan Region. Information on the catchment dynamics is scarce and no water resources management studies are available (UN-ESCWA and BGR 2013). Furthermore, water issues related to climate change in Khabour has been never addressed within climate change analyses and climate policy construction (Issa et al. 2014). This study aims to fill that gap.

To capture and describe these potential issues of the basin in a meaningful way, the physics–based Soil and Water Assessment Tool (SWAT) has been widely used for assessing climate change impacts on hydrological processes and nonpoint source pollution at various watershed scales (Arnold et al. 1998) was used in this study. The results of the research could make a significant contribution in providing a better understanding of the interaction between climate change and the hydrological system. This, in turn, will contribute towards better enabling humans adapting to the impacts of climate change and variability on water resources in Khabour Basin.

STUDIED AREA

Khabour (Figure 1) rises from the Eastern Anatolia Region in Turkey, flows to the south crossing Turkey-Iraqi border and then to the west through the Zakho City, finally it joins the Tigris River at a small distance to the south. The mean annual flow of Khabur is 68m^3/sec and its length is 181 km (UN-ESCWA and BGR 2013). Khabour River drains an area of 6,143 km^2, of which 43% situated in Iraq and 57% in Turkey. The basin is highly mountainous, with various elevations ranging from 300 to 3300 m above the sea level. Many springs rise in the basin. Mean annual temperature is 10°C and mean annual rainfall 780 mm. About 60% and 25% of precipitation including snowfall occurs in winter and spring, respectively. In autumn and summer, 14% and 1% of precipitation falls as rain, respectively. The flow regime of Khabour River demonstrates highly seasonal flow with peak flow occurring in May and low seasonal flow from July to December. This is a typical near-natural nival regime, in which winter precipitation in the form of snow and snow-melt in the spring is dominant. Approximately 46% of the watershed is covered by forest, 30% by Wetland-Forested and 23% of the land is used for agricultural activities. Up to date, no dams or regulators have been built on theKhabourRiver (UN-ESCWA and BGR 2013).

DESCRIPTION OF SWAT MODEL

The Soil and Water Assessment Tool (SWAT) model (Arnold et al. 1998) is a river watershed scale, semi-distributed and physically based discrete time (daily computational time step) model for analyzing hydrology and water quality at various watershed scales with varying soils, land use and management conditions on a long-term basis. The model was originally developed by the United States Department of Agriculture (USDA) and the Agricultural Research Service (ARS). SWAT system is embedded

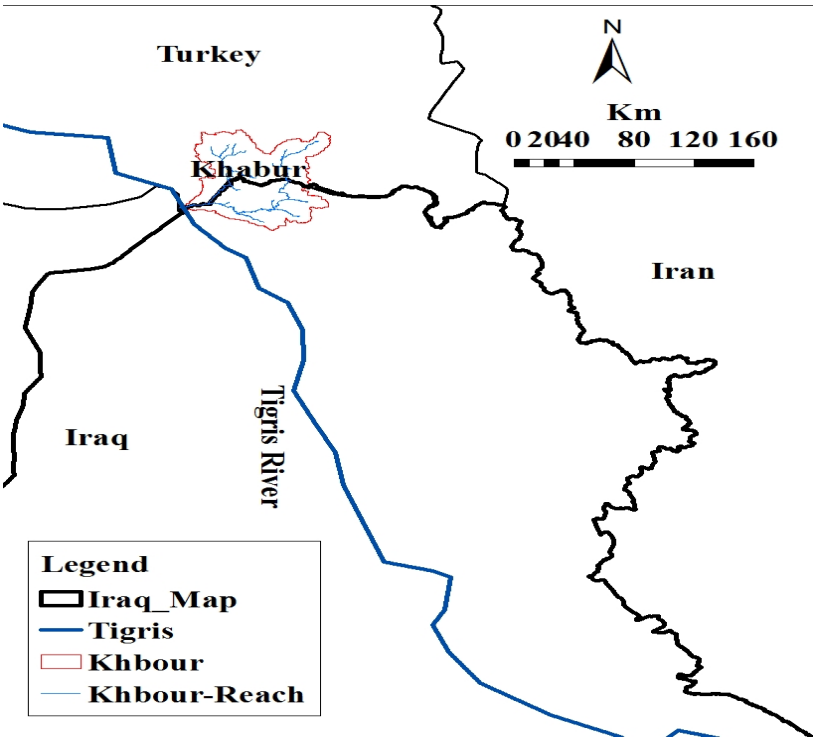

Figure 1. Location of Khabour Basin

within a Geographic Information System (ArcGIS interface), in which different spatial environmental data, including climate, soil, land cover and topographic characteristics can be integrated.

The model has two major divisions, land phase and routing phase, which are run to simulate the hydrology of a watershed. The land phase of the hydrological cycle predicts the hydrological components including surface runoff, evapotranspiration, groundwater, lateral flow, ponds, tributary channels and return flow. The routing phase of the hydrological cycles captures the movement of water, sediments, nutrients and organic chemicals via the channel network of the basin to the outlet.

In the land phase of the hydrological cycle, the simulation of the hydrological cycle is based on the water balance equation.

$$SW_t = SW_0 + \sum_{i=1}^{n} \left(R_{day} - Q_{surf} - E_a - W_{seep} - Q_{gw} \right) \quad (1)$$

where SW_t is the final soil water content (mm), SW_o is the initial soil water content on day i (mm), t is the time (days), R_{day} is the amount of precipitation on day i (mm), Q_{surf} is the amount of surface runoff on day i (mm), E_a is the amount of evapotranspiration on day i (mm), W_{seep} is the amount of water entering the vadose zone from the soil profile on day i (mm), and Q_{gw} is the amount of return flow on day i (mm). A brief description of some of the main components of the model is provided in this study, more detailed descriptions can be found in (Nietsch et al. 2005).

The estimation of surface runoff is done through two methods; the SCS curve number procedure (SCS 1972 in Arnold et al. 1998) and the Green and Ampt infiltration method (Green and Ampt 1911). The SCS method has been used in this study due to non-availability of sub-daily data that is required by the Green and Ampt infiltration method.

The SCS curve number equation is:

$$Q_{surf} = \frac{(R_{day} - 0.2S)^2}{(R_{day} + 0.8S)} \tag{2}$$

where, Q_{surf} is the accumulated runoff or rainfall excess (mm), R_{day} is the rainfall depth for the day (mm), S is the retention parameter (mm).

The retention parameter differs spatially owing to various soils; land use, management and slope within a catchment and temporally because of changes in soil water content. The retention parameter is defined by the equation;

$$S = 25.4\left(\frac{1000}{CN} - 10\right) \tag{3}$$

where CN is the curve number for the day.

SWAT offers two methods for estimating the retention parameter. The traditional method (soil moisture method) allows the retention parameter to be varied with soil profile water content. An alternative method added to SWAT 2012 is to allow the retention parameter to vary with accumulated plant evapotranspiration. The soil moisture method predicts too much runoff in shallow soils, but adding the calculation of daily CN value as a function of plant evapotranspiration, the value becomes less dependent on soil storage and more dependent on antecedent climate.

When the retention parameter is to be varied with soil profile water content, the following equation will be used,

$$S = S_1 max * \left(1 - \frac{SW}{[SW + \exp(w_1 - w_2 * SW)]}\right) \tag{4}$$

where S is the retention parameter for a given day (mm), S_{max} is the maximum value that the retention parameter can be achieved on any given day (mm), SW is the soil water content of the entire profile excluding the amount of water held in the profile at wilting point (mm), and w_1 and w_2 are shape coefficients. The maximum retention parameter value, S_{max}, is calculated by solving equation (3), using CN_1 as shown below,

$$S_{max} = 25.4\left(\frac{1000}{CN_1} - 10\right) \tag{5}$$

When the retention parameter differs with plant evapotranspiration, equation below is used to update the retention parameter at the end of every day:

$$S = S_{prev} + E_o \exp\left(\frac{-cncoef - S_{prev}}{S_{max}}\right) - R_{day} - Q_{surf} \quad (6)$$

where S_{prev} is the retention parameter for the previous day (mm), E_o is the potential evapotranspiration for the day (mm/day), *cncoef* is the weighting coefficient used to calculate the retention coefficient for daily curve number calculations which depend on plant evapotranspiration, S_{max} is the maximum value the retention parameter that can be achieved on any given day (mm), the R_{day} is the rainfall depth for the day (mm), and surf is the surface runoff (mm). The initial value of the retention parameter is defined as $S = 0.9S_{max}$.

The model estimates the volume of lateral flow depending on the variation in conductivity, slope and soil water content. A kinematic storage model is utilized to predict lateral flow through each soil layer. Lateral flow occurs below the surface when the water rates in a layer exceed the field capacity after percolation.

As to groundwater simulation, the process is structured into two aquifers which are a shallow aquifer (unconfined) and a deep aquifer (confined) in each watershed. The shallow aquifer contributes to stream flow in the main channel of the watershed.

The water balance equation for the shallow aquifer is:

$$aq_{sh,i} = aq_{sh,i-1} + w_{rchg.sh} - Q_{gw} - w_{revap} - w_{pump.sh} \quad (7)$$

where aq_{shi} is the amount of water stored in the shallow aquifer on day i (mm), $aq_{sh,i-1}$ is the amount of water stored in the shallow aquifer on day i-1 (mm), $w_{rchrg.sh}$ is the amount of recharge entering the aquifer on day i (mm), Q_{gw} is the groundwater flow, or base flow, into the main channel on day i (mm), w_{revap} is the amount of water moving into the soil zone in response to water deficiencies on day i (mm), and $w_{pump,sh}$ is the amount of water removed from the shallow aquifer by pumping on day i (mm).

The steady-state response of groundwater flow to recharge is calculated by the equation below (Hooghoudt 1940 in Arnold et al. 2005).

$$Q_{gw} = \frac{8000 * K_{sat}}{L_{gw}^{\ 2}} * h_{wtbl} \quad (8)$$

where K_{sat} is the hydraulic conductivity of the aquifer (mm/day), L_{gw} is the distance from the ridge or sub-basin divide for the groundwater system to the main channel (m), and h_{wtbl} is the water table height (m).

Water that percolates into the confined aquifer is presumably contributing to stream flow outside the watershed. Three methods are provided by SWAT model to estimate potential evapotranspiration (PET) – the Penman-Monteith method (Monteith 1965), the Priestley-Taylor method (Priestley and Taylor 1972) and the Hargreaves method (Hargreaves et al. 1985). Water is routed through the channel network by applying either the variable storage routing or Muskingum river routing methods using the daily time step.

MODEL INPUT

Huge amount of input data is required by SWAT model to fulfil the tasks envisaged in this research. Basic data requirements for modelling included digital elevation model (DEM), land use map, soil map, weather data and discharge data. DEM was extracted from ASTER Global Digital Elevation Model (ASTERGDM) with a 30 meter grid and 1×1 degree tiles (http://gdem.ersdac.jspacesystems.or.jp/tile_list.jsp). The land cover map was obtained from the European Environment Agency (http://www.eea.europa.eu/data-and-maps/data/global-land-cover-250m) with a 250 meter grid raster for the year 2000. The soil map was collected from the global soil map of the Food and Agriculture Organization of the United Nations (1995). Weather data included daily precipitation, 0.5 hourly precipitation, maximum and minimum temperatures obtained from the Iraq's Bureau of Meteorology. Monthly stream flow data was collected from the Iraqi Ministry of Water Resources/National Water Centre.

Model setup

In SWAT model, the watershed is subdivided into small basins based on the digital elevation model (DEM). The land use map, soil map and slope datasets were embedded with the SWAT databases in this study. Thereafter, the small basins are further drilled down by Hydrologic Response Units (HRUs). HRUs are defined as packages of land that have a unique slope, soil and land use area within the borders of a small basin. The HRUs represent percentages of a sub-basin area and hence are not spatially defined in the model. There must be at least one HRU in each basin. HRUs enable the user to identify the differences in hydrologic conditions such as evapotranspiration for varied soils and land uses. Routing of water and pollutants are predicted from the HRUs to the sub-basin level and then through the river system to the watershed outlet.

Model calibration and evaluation

To evaluate the performance of the SWAT model, the sequential uncertainty fitting algorithm application (SUFI-2) embedded in the SWAT-CUP package (Abbaspour et al. 2007) was used. The advantages of SUFI-2 are that it combines optimization and uncertainty analysis, can handle a large number of parameters through Latin hypercube sampling and it is easy to apply. Furthermore, as compared with different techniques in connection to SWAT such as generalized likelihood uncertainty (GLU) estimation, parameter solution (parsol), Markov Chain Monte Carlo (MCMC), SUFI-2 algorithm was found to obtain good prediction uncertainty ranges with a few numbers of runs. This efficiency is of great significance when implementing complex and large-scale models (Abbaspour et al. 2004).

The SUFI-2 first identifies the range for each parameter. After that, Latin Hypercube method is used to generate multiple combinations among the calibration parameters. Finally, the model runs with each combination and the obtained results are compared with observed data until the optimum objective function is achieved. Since the uncertainty in forcing inputs (e.g. temperature, rainfall), conceptual model and measured data are not avoidable in hydrological models, the SUFI-2 algorithm computes the uncertainty of the measurements, the conceptual model and the parameters by two measures: P-factor and R-factor. P-factor is the percentage of data covered by the 95% prediction uncertainty (PPU) which is quantified at 2.5% and 97.5% of the cumulative distribution of an output variable obtained through Latin Hypercube Sampling. The R-factor is the average width of the 95 PPU divided by the standard deviation of the corresponding measured variable. In an ideal situation, P-factor tends towards 1 and R-factor to zero. Further, SUFI-2 calculates the Coefficient of Determination (R^2) and the Nasch-Sutcliff

efficiency (ENC) (Nash and Sutcliffe 1970) to assess the goodness of fit between the measured and simulated data.

The ENC value is an indication of how well the plot of the observed against the simulated values fits the 1:1 line. It can range from negative infinity (-∞) to one. The closer the value to one, the better is the prediction, while the value of less than 0.5 indicates unsatisfactory model performance (Moriasi et al. 2007). ENC is calculated as shown below:

$$ENC = 1 - \left[\frac{\sum_{i=1}^{n} (O_i - P_i)^2}{\sum_{i=1}^{n} (O_i - \acute{O})^2} \right] \tag{9}$$

where O_i is the observed stream flow, P_i is the simulated stream flow and $\bar{O}$ is the mean observed stream flow during the evaluation period.

ENC was recommended to be used for calibration for two reasons. First, it has been adopted by ASCE (1993) and second, Legates and McCabe (1999) recommend it due to its straightforward physical interpretation (Raghavan et al. 2014). Besides, it has found wide applications offering extensive information on reported values (Moriasi et al. 2007).

SUFI-2 enables users to conduct global sensitivity analysis, which is computed based on the Latin Hypercube and multiple regression analysis. The multiple regression equation is defined as below.

$$g = \alpha + \sum_{i=1}^{m} \beta_i * b_i \tag{10}$$

where g is the value of evaluation index for the model simulations, α is a constant in multiple linear regression equation, β is a coefficient of the regression equation, b is a parameter generated by the Latin hypercube method and m is the number of parameters.

The *t*-stat of this equation which indicates parameter sensitivity is applied to determine the relative significance for each parameter, the more the sensitive parameter, greater is the absolute value of the *t*-stat. When *p*-value is used, it is an indication of the significance of the sensitivity, *p*-value close to zero has more significance.

General Circulation Model (GCM) inputs

Six GCMs from CMIP3 namely CGCM3.1/T47, CNRM-CM3, GFDL-CM2.1, IPSLCM4, MIROC3.2 (medres) and MRI CGCM2.3.2 were selected for climate change projections in the Khabour basin under a very high emission scenario (A2), a medium emission scenario (A1B) and a low emission scenario (B1) for two future periods (2046-2064) and (2080-2100). The projected temperatures and precipitation were then input to the SWAT model to compare water resources in the basin with the baseline period (1980-2010). Fig. 2 provides the information for the baseline period. BCSD method was used to downscale the GCM results (Maurer et al. 2014).

RESULTS

Global sensitivity

An initial sensitivity analysis was applied prior to calibrating the model to examine the sensitivity of different parameters related to stream flow (Table 1). The results show that SUFI-2 has been able to identify the most influential parameters on the model results. In the current study, sensitivity analysis has been carried out for 25 parameters related to stream flow (Table 1), from which 12 most sensitive parameters have been considered (Table 2) for implementing the calibration.

Table 1. Description of input parameters of stream flow selected for model calibration.

Group	Parameter	Description	Unit
Soil	SOL_ALB	Moist soil albedo	-
	SOL_AWC	Available water capacity	mm mm^{-1}
	SOL_K	Saturated hydraulic conductivity	mmh^{-1}
	SOL_Z	Depth to bottom of second soil layer	mm
Groundwater	ALPHA_BF	Base flow Alpha factor	days
	GW_DELAY	Groundwater delay	days
	GW_REVAP	Groundwater 'revap' coefficient	-
	GWQMN	Threshold depth of water in the shallow aquifer for return flow to occur	mm H_2O
	REVAPMN	Threshold depth of water in the shallow aquifer for 'revap' to occur	mm H_2O
Subbasin	TLAPS	Temperature laps rate	°C km^{-1}
HRU	EPCO	Soil evaporation compensation factor	-
	ESCO	Plant uptake compensation factor	-
	CANMX	Maximum canopy storage	mm H_2O
	SLSUBBSN	Average slope length	m
Routing	CH_N2	Manning's n value for the main channel	-
	CH_K2	Effective hydraulic conductivity in main channel alluvium	mm h^{-1}
Management	BIOMIX	Biological mixing efficiency	-
	CN2	Initial SCS runoff curve number for moisture condition II	-
General data basin	SFTMP	Snowfall temperature	°C
	SMFMN	Minimum melt rate for snow during year	mm H_2O °C^{-1} day^{-1}
	SMFMX	Maximum melt rate for snow during year	mm H_2O °C^{-1} day^{-1}
	TEMP	Snow pack temperature lag factor	-
	SURLAG	Surface runoff lag time	days
	BLAI	Maximum potential leaf area index for land cover/plant	-
	SLOPE	Slope	-

This table is adapted from (Arnold et al. 1998)

Table 2. Ranking of 12 highest sensitive parameters related to stream flow in the five basins.

Parameter	Rank	Initial values	Fitted values
SFTMP	1	-5 – 5	3.68
CN2	2	-0.2 – 0.2	0.02
ALPHA_BF	3	0 – 1	0.182
GW_DELAY	4	30 – 450	183
SLSUBBSN	5	0 – 0.2	0.145
SOL_AWC	6	-0.2 – 0.4	0.342
CH_K2	7	5 – 130	73
GWQMN	8	0 – 2	1.23
GW_REVAP	9	0 – 0.2	0.09
SURLAG	10	0.05 – 24	16.8
ESCO.hru	11	0 – 0.2	0.067
HRU_SLP	12	0 – 0.2	0.12

SFTMP was the dominant SWAT calibration parameter for the Khabour basin. This is a reasonable result as Khabour basin is classified as snow-dominated mountainous basin. CN2 was the second influential parameter. In most SWAT applications in different watersheds CN2 was found to be the most sensitive parameter (Cibin et al. 2010). ALPHA-BF was ranked as the second. This result is consistent with the finding of Li et al. (2009), who found that ALPHA is highly sensitive groundwater parameter in SWAT calibration.

Calibration and validation

The model was calibrated and validated at the solo discharge station, Zakho station which is located at Latitude 37° 08′ 00″ N, Longitude 42° 41′ 00″ E, near to the Khabour basin outlet. The calibration period was ten years (1977-1986) and the validation period was three years (1987-1999). The first three years was warm up period. The results of flow calibration of the Zakho monitoring station showed a good agreement between observed and simulated values (Figure 2). R^2 value was 0.50 and ENC index was 0.51. In addition, 45% of observed data was bracketed by 95 PPU (P-factor) with R-factor of 1.89. During the validation, R^2 and ENC remained nearly consistent, P- factor increased to 0.75 and R-factor decreased to 1.56.

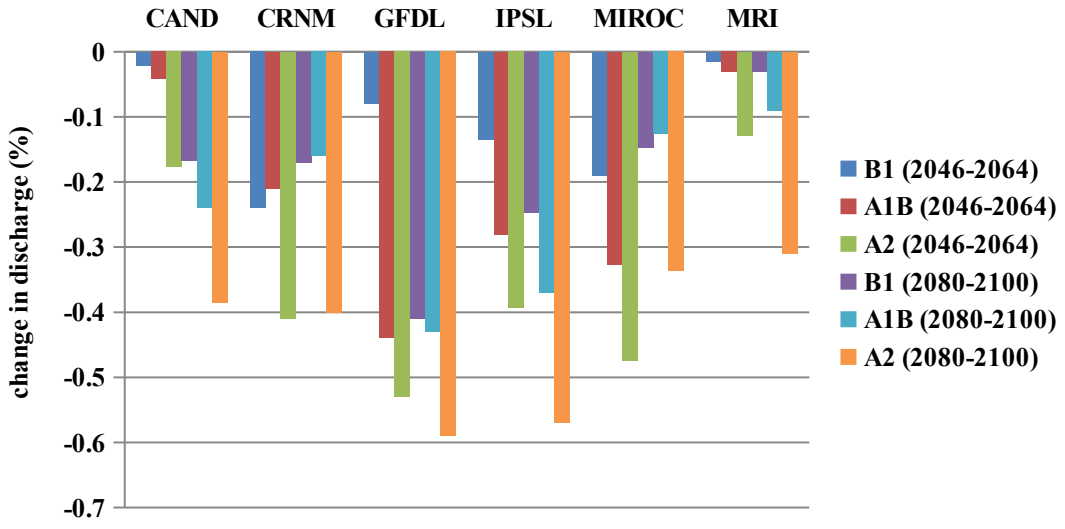

Figure 2. Calibration and validation of the SWAT model at monthly scale at Zakho station.

Trends in precipitation, blue water and green water in the past

Using the calibrated model, annual precipitation, blue water (summation of water yield and deep aquifer recharge) and green water including green water storage (soil water content) were estimated during the last three decades to identify the impacts of climate change on the water cycle components. Blue water is the freshwater humans can access for in stream use or withdrawal. Green water does not provide direct access to humans but sustains natural flora and rain-fed agriculture.

The spatial distribution of precipitation in HRUs over three consecutive decades is shown in Figure 3. From the figure it appears that there is a general decreasing trend in precipitation over time.

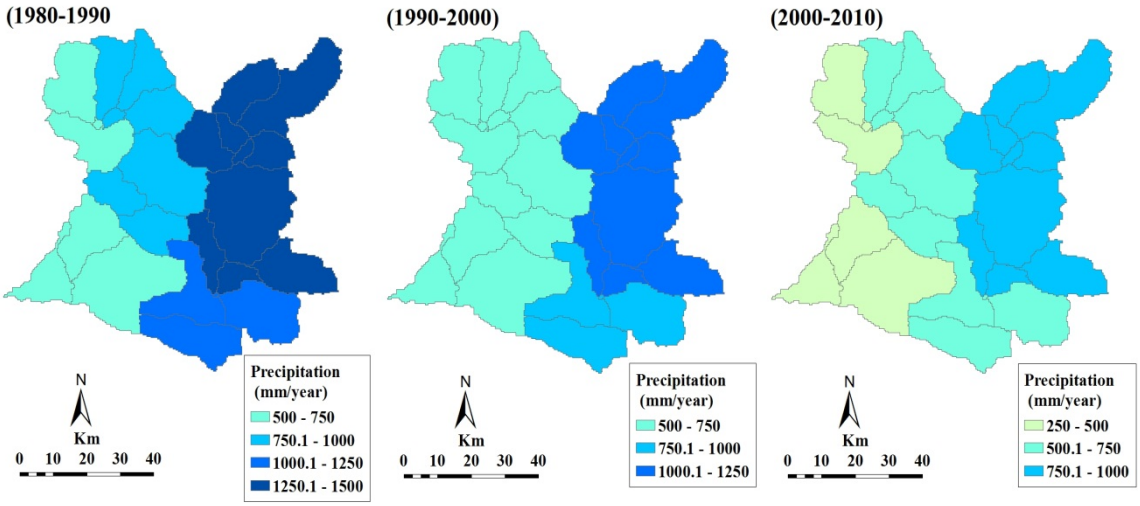

Figure 3. Spatial distribution of precipitation in the Khabour basin over three consecutive decades.

Spatial distribution of blue water and green water in the Khabour basin are shown in Figures 4 and 5. The spatial patterns of the blue and green water flows are largely affected by the spatial patterns of precipitation. In addition, land cover contributes to the shaping of spatial patterns. Generally, green water tracks blue water, where blue water flows are high, green water flows also have a tendency to be high. The average annual blue water and green water for the entire catchment significantly decreased from 1980s to 2000s. It is plausible that the decreasing trends in the average annual blue water and green water are attributable to climate change. Green water flow stayed nearly consistent due to hypothesis that the land cover stayed consistent through the period of (1980-2010). Table 3 provides numerical values of relative changes.

The calibrated model was also applied for blue water scarcity analysis. The five water stress ranks introduced in Figure 7 follow the most widely applied water stress indicators defined by Falkenmark et al. (1989) and Rijsberman (2006). The water stress threshold defined as 1700 $m^3.capita^{-1}.year^{-1}$. The 1700 $m^3.capita^{-1}.year^{-1}$ is calculated based on estimations of water needs in the household, agricultural, industrial and energy sectors, and the demand of the environment (Rijsberman 2006). A value equal or greater than 1700 $m^3.capita^{-1}.year^{-1}$ is considered as adequate to meet water demands. When water supply drops below 1000 $m^3.capita^{-1}.year^{-1}$ it is referred to as water scarcity, while a value below 500 $m^3.capita^{-1}$. $year^{-1}$ is considered as extreme scarcity.

The water availability per capita and water stress indicators were estimated for each of the 27 sub-basins of the Khabour catchment using the 2.5 arcmin population map available from the Center for

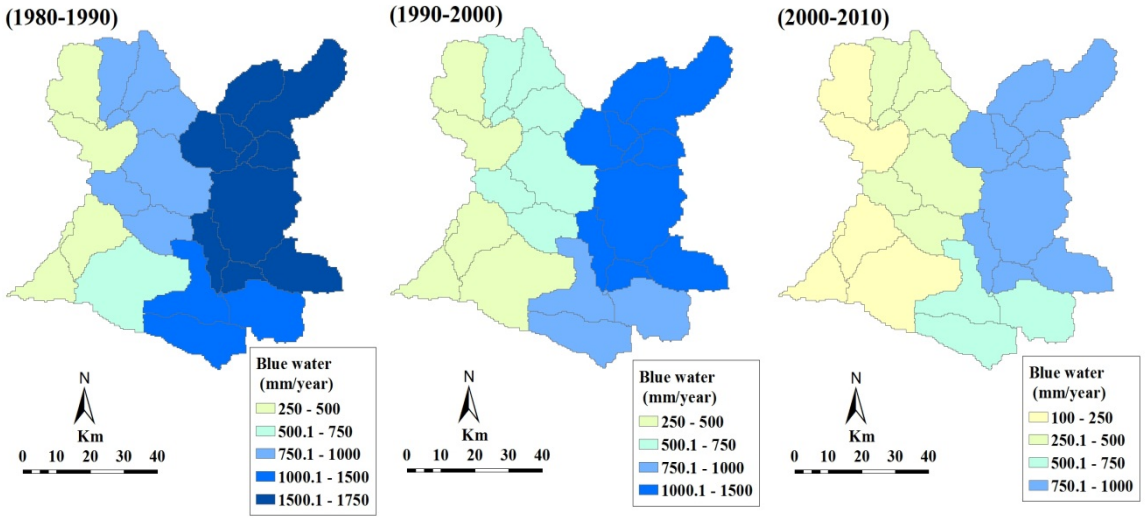

Figure 4: Spatial distribution of blue water in the Khabour basin over three consecutive decades.

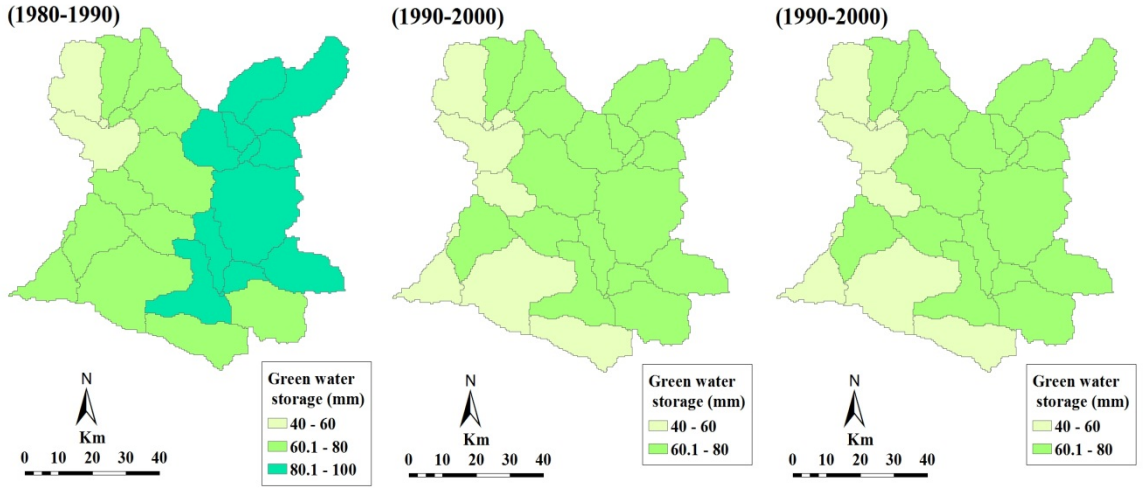

Figure 5: Spatial distribution of green water storage in the Khabour basin over three consecutive decades.

Table 3: Relative changes in precipitation, blue water and green water in theKhabourbasin over three decades.

	Rate of relative change in the last three decades		
Water component	1990s vs 1980s	2000s vs 1990s	2000s vs 1980s
Precipitation	-0.14	-0.31	-0.40
Blue water	-0.22	-0.47	-0.60
Green water storage	-0.12	-0.08	-0.20
Green water flow	-0.04	-0.05	-0.04

Blue water scarcity indicators

International Earth Science (CIESIN) Gridded Population of the World (GPW, version 3, http://sedac.ciesin.columbia. edu/gpw) for 2005. Fig. 7 demonstrates the spatial distribution of water resources per capita per year during the period of 1980-2010 based on the population estimates of the year of 2005. In general, 7% of the basin located mostly in the lower part of the basin suffers blue water scarcity (less than 500 m^3/capita.year. Up to 21% of the basin area, located in the upper part of the basin, experiences sufficient water (more than 2 500 m^3/capita.year). Thirty nine percent of the basin experiences greater than 1700 m^3/capita.year and lesser than 2500 m^3/capita.year. It is clearly seen that most of the Khabour basin has sufficient water.

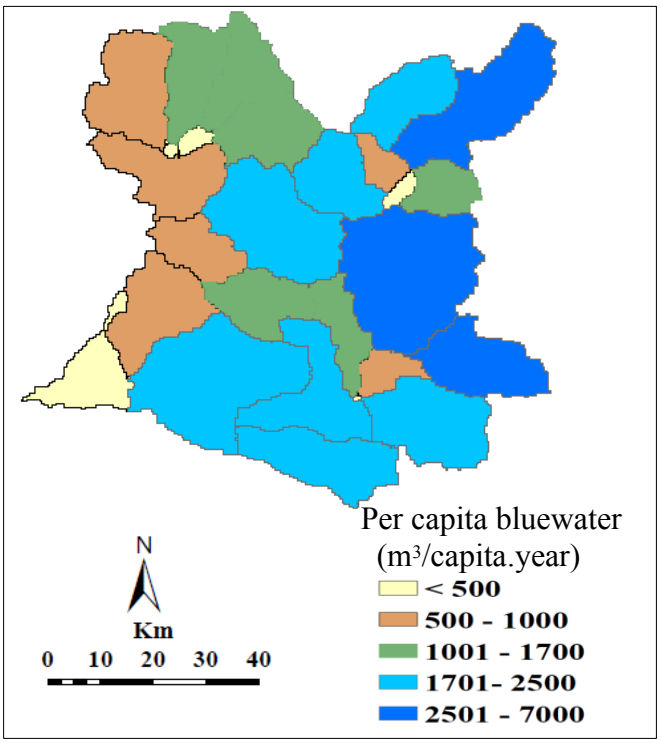

Figure 6. Water scarcity in each Khabour sub-basin captured by 1980-2010 annual average blue water flow availability per capita per year (using population of 2005) applying the average value of the 95 PPU range.

Uncertainty and natural variation in green water storage

For the rainfed crops, the average of the months per year for the period of 1980 to 2010 where green water storage is available (defined as >1 mm m^{-1}) is of greatest significance (Zang et al. 2012). This is shown in Fig. 7 (left). Up to 77% of the basin experiences 8 to 9 months (September to May) in which green water is available .The standard deviation (SD) of the months per year without depleted soil water is presented for the 1980–2010 period in Fig. 7 (right). The areas with a high SD located in north east and middle of the basin show high variability in green water storage availability. This might cause a reduction in crop yield or crop loss. Adjustment of irrigation systems and adoption of alternative cropping practices could be recommended in these lands to sustain agriculture production.

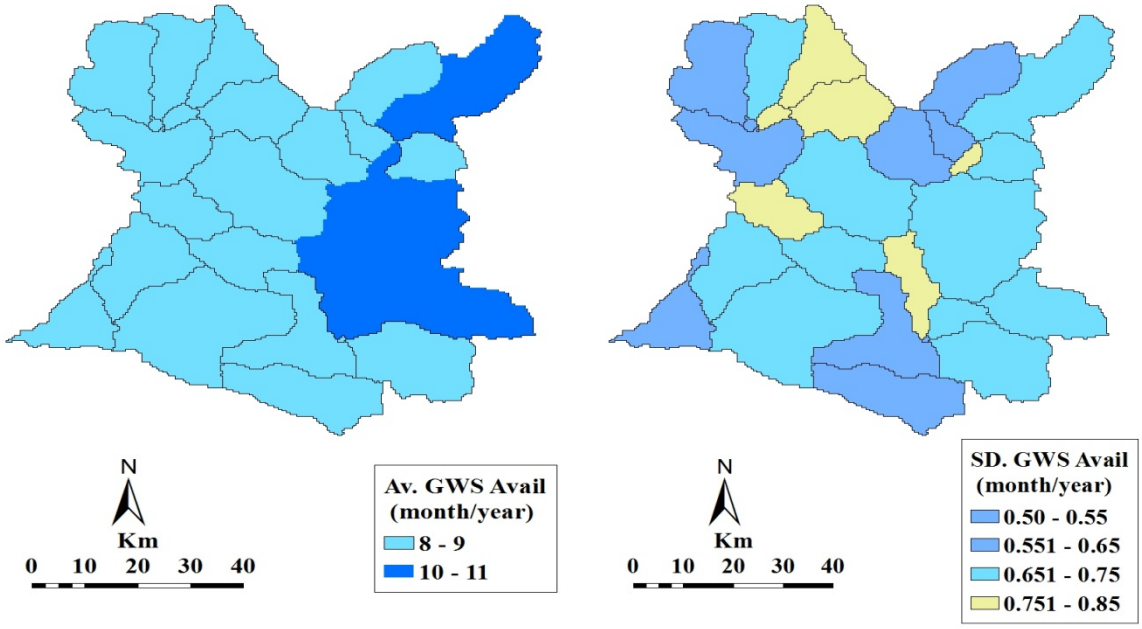

Figure 7. (Right) The 1980–2010 average green water and (Left) standard deviation (SD) of the number of months per year where the green water storage (GWS) is available for usage.

The impacts of climate change on temperature and precipitation under A2, A1B, B1 emission scenarios

Mean annual temperature and precipitation outputs from the six GCMs identified earlier were processed for the Khabour basin under three scenarios (A2, A1B, B1). Table 4 captures the projected changes in mean annual temperature for two future periods (2046-2064) and (2080-2100) relative to base period (1980-2010). All scenarios projected increases in mean temperature. GFDL predicted the greatest increases in temperature and MRI projected the lowest temperatures

Table 4. GCM predicted changes in the mean annual temperature of the future under A2, A1B and B1 scenarios.

Periods	Annual change in min temperature (^{0}C)					
	CGCM3.1/T47	CNRM-CM3	GFDL-CM2.1	PSLCM4	MIROC3.2	MRI CGCM2.3.2
A2						
2046-2064	2.8	2.6	2.5	2.1	2.5	1.7
2080-2100	5.3	5	5.3	4.3	4.5	3.6
A1B						
2046-2064	2.5	2.3	3	2.7	2.3	2
2080-2100	4.0	3.5	4.5	3.6	4.2	3.2
B1						
2046-2064	1.4	1.4	1.5	1.3	1.4	1.3
2080-2100	1.5	1.2	1.5	1.5	1.5	1.3

Table 5 captures the relative changes in precipitation for near future (2046-2064) and distant future (2080-2100) relative to base line period (1980-2010). All scenarios projected decreases in precipitation

for both periods. GFDL-CM2.1 projected the highest reduction under three emission scenarios; however, MRI CGCM2.3.2 predicted the lowest reduction in precipitation.

Table 5. GCM predicted changes in the mean annual precipitation of the future under A2, A1B and B1 scenarios.

Periods	Annual change in precipitation (%)					
	CGCM3.1/T47	CNRM-CM3	GFDL-CM2.1	PSLCM4	MIROC3.2	MRI CGCM2.3.2
A2						
2046-2064	-0.09	-0.08	-0.18	-0.11	-0.12	-0.07
2080-2100	-0.22	-0.22	-0.38	-0.35	-0.28	-0.25
A1B						
2046-2064	-0.07	-0.16	-0.13	-0.12	-0.16	-0.09
2080-2100	-0.17	-0.18	-0.26	-0.24	-0.23	-0.15
B1						
2046-2064	0.02	-0.04	-0.07	-0.06	-0.04	-0.01
2080-2100	-0.09	-0.06	-0.15	-0.05	-0.07	-0.04

Fig. 8 shows the anomaly maps of blue water distribution (maps of percent deviation from historic data, 1980-2010) for A2, A1B and B1 scenarios for the periods 2046-2064 and 2080-2100 for the average change of multi-GCM ensemble. The A2 scenario projected the mean reduction for the whole basin (12%) followed by A1B (11%) and then B1 (3%). In the centennial future, the reduction would increase to 27%, 22% and 7% under A2, A1B and B1, respectively.

The impacts of climate change on blue and green water under A2, A1B, B1 emission scenarios

Fig. 9 shows the anomaly maps of blue water distribution (maps of percent deviation from historic data, 1980-2010) for A2, A1B and B1 scenarios for the periods 2046-2064 and 2080-2100 for the average change of multi-GCM ensemble. The half-centennial projection (2046-2064) and centennial future (2080-2100) show a decrease in blue water under all emission scenarios for the whole basin. A2 scenario projected the mean reduction for the whole basin (26%) followed by A1B (17%) and then B1 (7%) for the period 2046 to 2064. In the centennial future, the reduction would increase to 43%, 37% and 17% under A2, A1B and B1, respectively. Similarly, green water flows would decrease under the three emission scenarios for the two future periods (Figure 10).

Impacts of climate change on deep aquifer recharge

Figure 11 captures the anomaly maps of deep aquifer recharge distribution (maps of percent deviation from historic data, 1980-2010) for A2, A1B and B1 scenarios for the periods 2046-2064 and 2080-2100 for the average change of multi-GCM ensemble. All scenarios in the near and far future indicated that the basin will experience decreases in ground water recharge. The A2 scenario projected the mean decrease for the whole basin (28%) followed by A1B (25%) and then B1 (6%) for the period 2046 to 2064. In the far future, the reduction would increase to 45%, 39% and 17% under A2, A1B and B1.

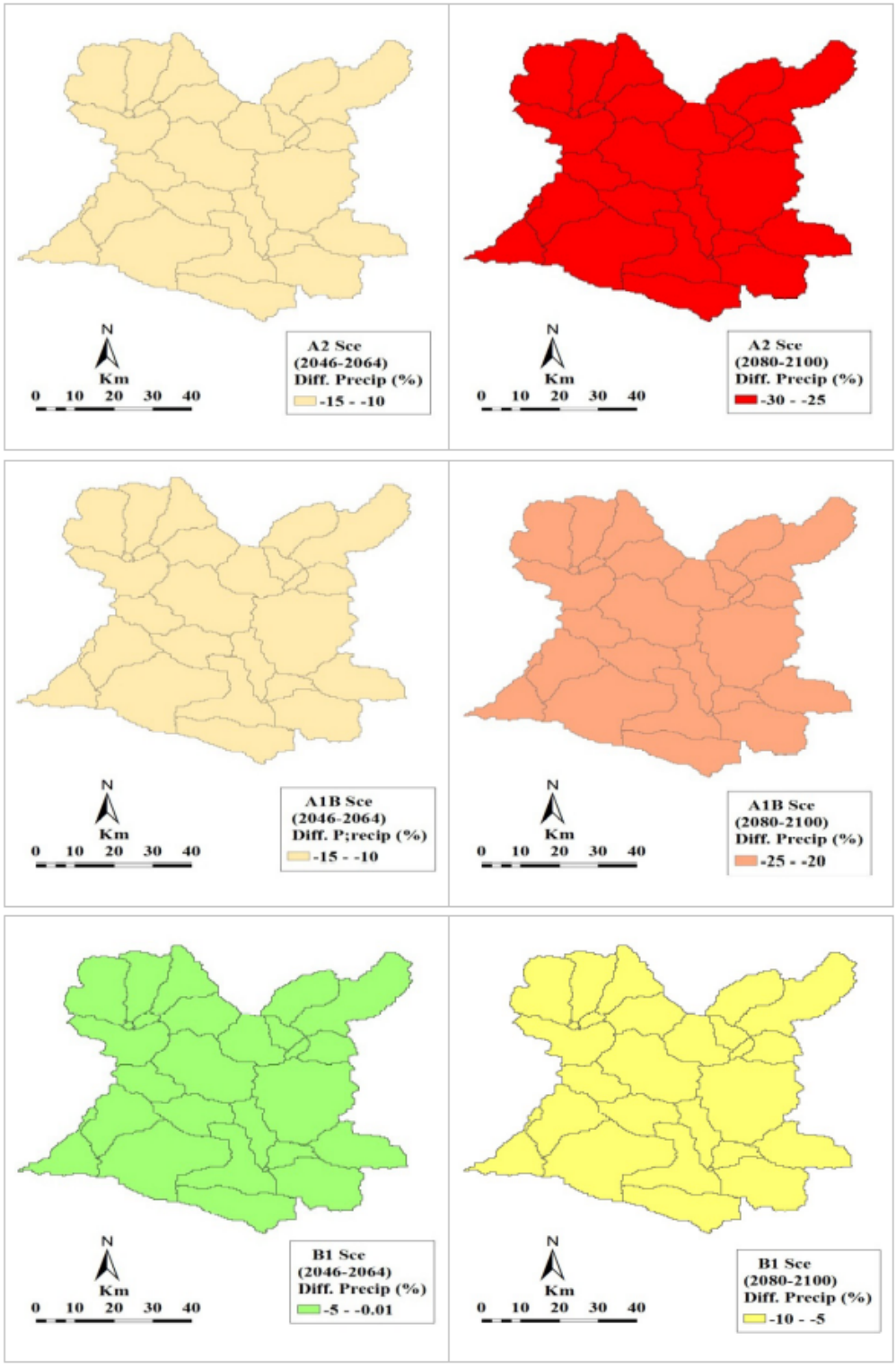

Figure 8. The impacts of climate change on the precipitation of the basin based on scenarios A2, A1B, and B1 for periods 2046-2064 and 2080–2100.

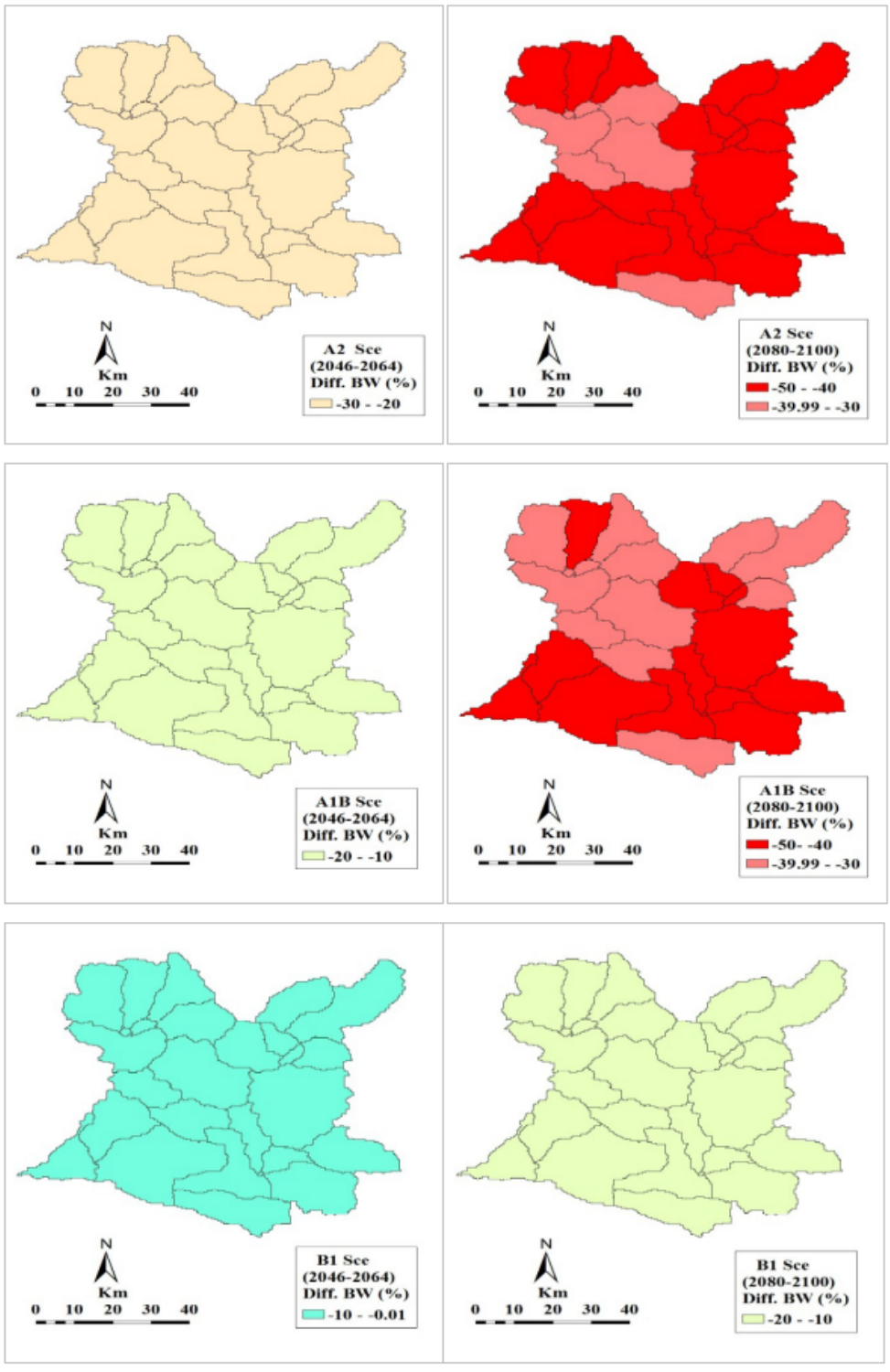

Figure 9. The impacts of climate change on the blue water of the basin based on scenarios A2, A1B, and B1 for periods 2046-2064 and 2080–2100.

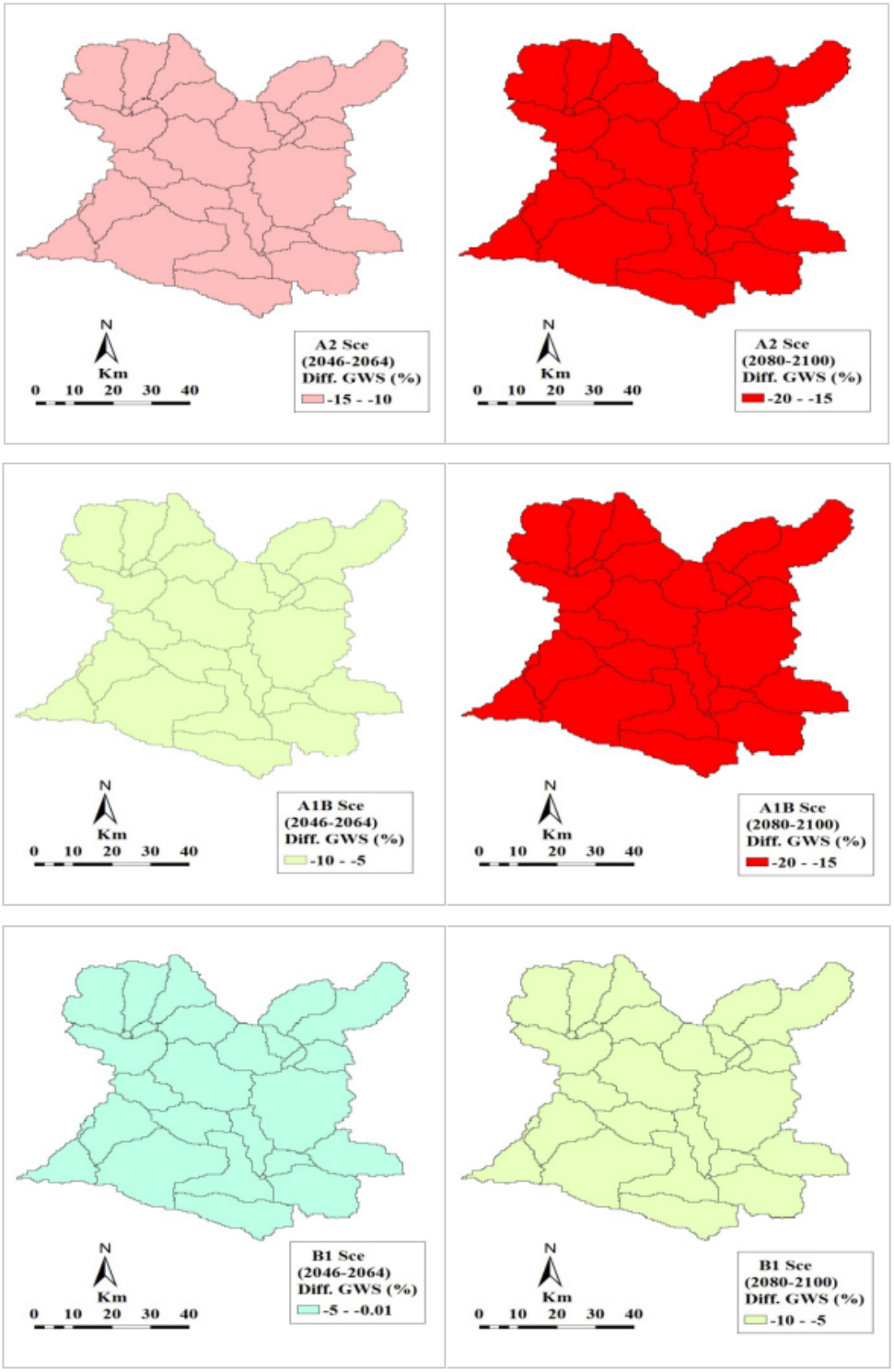

Figure 10. The impacts of climate change on the green water storage of the basin based on scenarios A2, A1B, and B1 for periods 2046-2064 and 2080–2100.

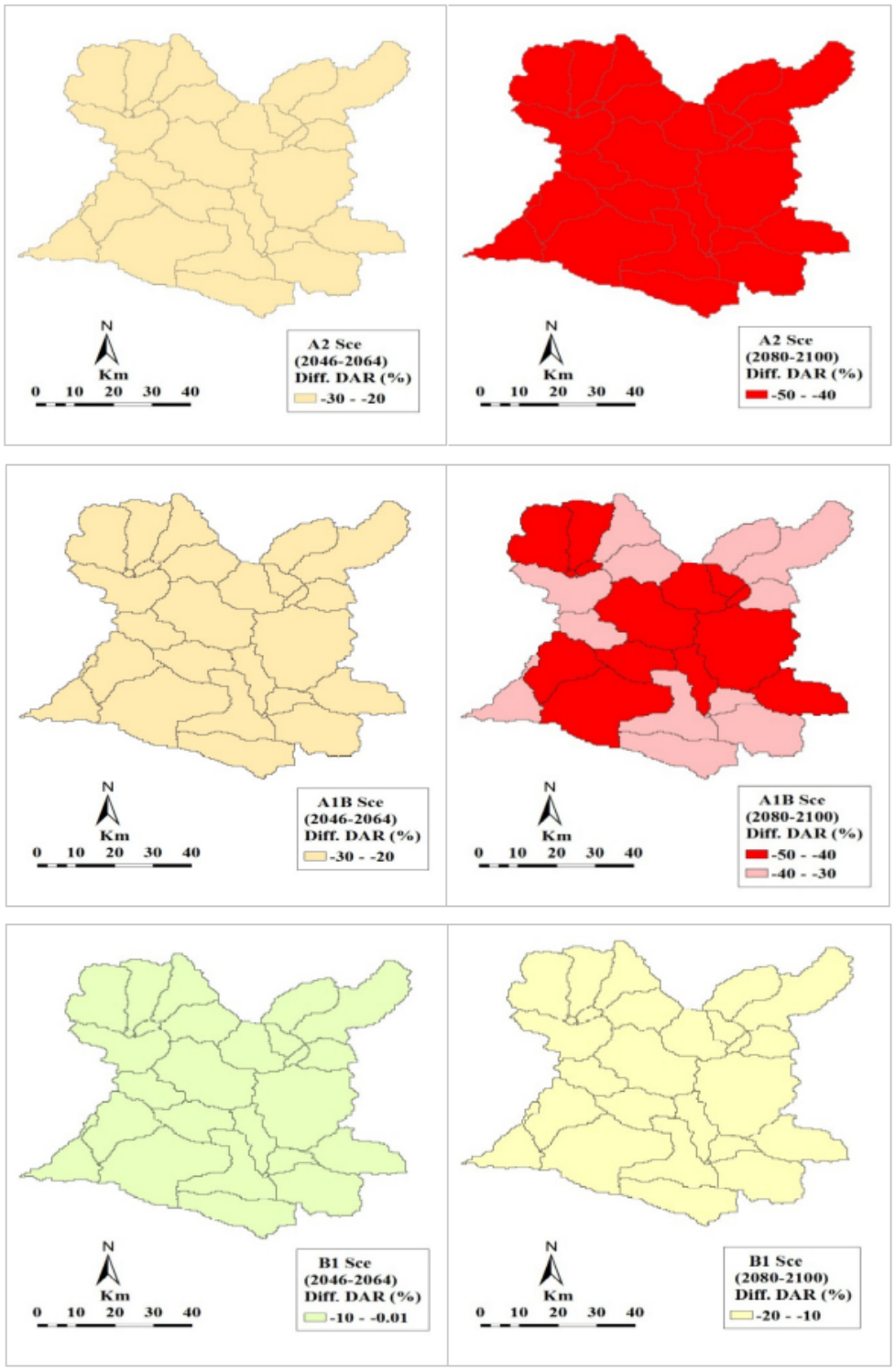

Figure 11. The impacts of climate change on the deep aquifer recharge of the basin based on scenarios A2, A1B, and B1 for periods 2046-2064 and 2080–2100.

Impacts of climate change on stream flow

Flow discharge is a significant hydrological element, and is significantly impacted by precipitation. Figure 12 captures the projected effect of climate change on annual stream flow. Using downscaled data from the Six GCMs, CGCM3.1/T47, CNRM-CM3, GFDL-CM2.1, IPSLCM4, MIROC3.2 (medres) and MRI CGCM2.3.2 , the streamflow showed decreases under all emission scenarios for both time period (2046-2064 and 2080-2100). GFDL model projected a greatest reduction under the three emissions scenarios (A2, A1B, B1) for both periods. MRI CGCM2.3.2 model, however, projected the lowest reductions in streamflow.

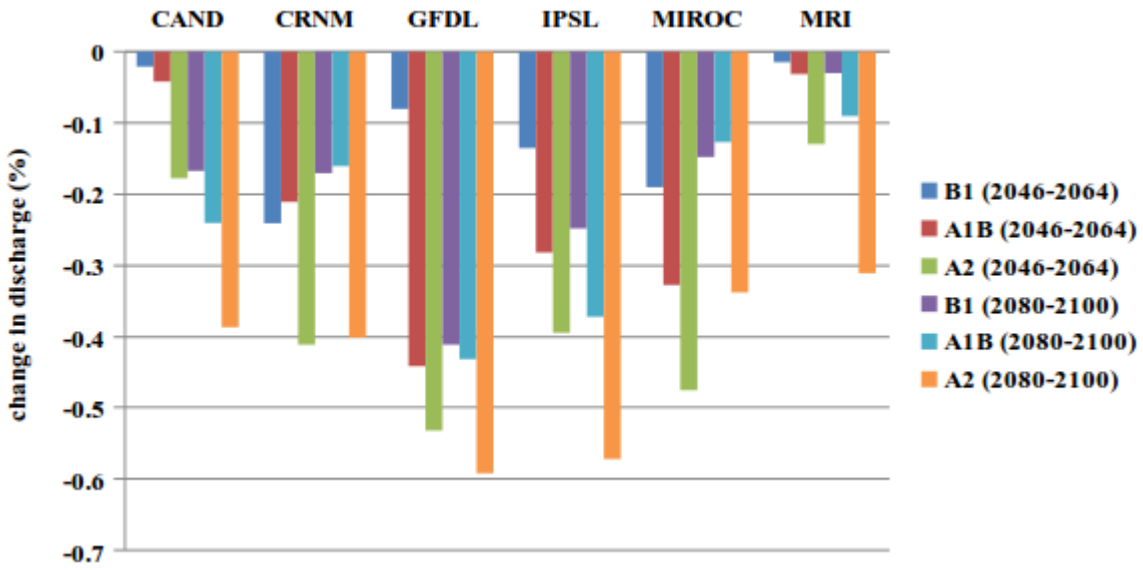

Figure 12. Change in annual streamflow due to changes in precipitation and temperature under A2, A1B and B1 scenarios for CGCM3.1/T47, CNRM-CM3, GFDL-CM2.1, IPSLCM4, MIROC3.2 (medres) and MRI CGCM2.3.2 the periods 2046-2064 and 2080-2100 expressed as a percentage of streamflow in the base period 1980-2010.

CONCLUSION

The SWAT model was applied to the Khabour basin at monthly time steps. The model was calibrated and validated at the solo Zakho discharge station to simulate the stream flow. The performance of the model was found to be rather good with R^2 and ENC indices during the calibration and validation periods. The calibrated model was used for identifying the trends of water components in the last three decades. Precipitation, blue water, and green water flows were found to significantly decrease from 1980 to 2010. The findings matched with observations. Next, the model was applied for assessing the impacts of climate change in near future (2046-2064) and distant future (2080-2100) under three emission scenarios (A2, A1B, B1) using six GCMs. All model runs under three emission scenarios predicted that the catchment will be drier in the near and distant futures. The results of this study could be advantageous in detecting appropriate water resources management strategies and cultivation practices for the future.

ACKNOWLEDGMENTS

The authors would like to express their thanks to Professors Rafid Alkhaddar of Liverpool JM University, UK, Professor Mustafa Alshawi of Salford University, UK, and Professor Kadhium Almuqdadi of the Arab Academy, Denmark for reviewing the manuscript and their fruitful discussions.

REFERENCES

Abbaspour, K., C. Johnson and M. T. Van Genuchten (2004). "Estimating uncertain flow and transport parameters using a sequential uncertainty fitting procedure." Journal of Vadose Zone, vol. 3, no.4, pp. 1340-1352.

Abbaspour, K.C., J. Yang, I. Maximov, R. Siber, K. Bogner, J. Mieleitner, J. Zobrist and R. Srinivasan, 2007. Modelling Hydrology and Water Quality in the Pre-Alpine/Alpine Thur Watershed using SWAT. Journal of Hydrology, 333(2-4): 413-430. doi:10.1016/j.jhydrol.2006.09.014.

Al-Ansari, N., A. A. Ali and S. Knutsson (2014). "Present Conditions and Future Challenges of Water Resources Problems in Iraq." Journal of Water Resource and Protection, vol. 6, pp 1066-1098.

Arnold, J.G., R. Srinivasan, R.S. Muttiah and J.R. Williams, 1998. Large Area Hydrologic Modeling and Assessment Part I: Model Development, Wiley Online Library.

Cibin, R., K. Sudheer and I. Chaubey (2010). "Sensitivity and identifiability of stream flow generation parameters of the SWAT model." Hydrological processes 24(9): 1133-1148.

Falkenmark, M. (1989). "The massive water scarcity now threatening Africa: why isn't it being addressed?" Ambio: 112-118.

Green, W. H. and G. Ampt (1911). "Studies on soil physics, 1. The flow of air and water through soils." Journal of Agriculture Science, vol. 4, pp. 1-24.

Hargreaves, G.L., G.H. Hargreaves, J. Riley, 1985. Agricultural Benefits for Senegal River Basin. Journal of irrigation and Drainage Engineering, 111(2): 113-124.

Issa, I.E., N.A. Al-Ansari, G. Sherwany and S. Knutsson, 2014. Expected Future of Water Resources within Tigris-Euphrates Rivers Basin, Iraq. Journal of Water Resource and Protection, 6: 421-432.

Legates, D. R. and G. J. McCabe (1999). "Evaluating the use of "goodness□of□fit" measures in hydrologic and hydroclimatic model validation." Journal of Water resources research, vol. 35, no.1,pp. 233-241.

Li, Z., Z. Xu, Q. Shao and J. Yang (2009). "Parameter estimation and uncertainty analysis of SWAT model in upper reaches of the Heihe river basin." Hydrological Processes 23(19): 2744-2753.

Maurer, E., L. Brekke, T. Pruitt, B. Thrasher, J. Long, P. Duffy, M. Dettinger, D. Cayan and J. Arnold (2014). "An Enhanced Archive Facilitating Climate Impacts and Adaptation Analysis." Bulletin of the American Meteorological Society 95(7): 1011-1019.

Monteith, J. (1965). Evaporation and the environment, the state and movement of water in living organisms. XIXthe Symposium, Cambridge University Press, Swansea.

Moriasi, D.N., J.G. Arnold, M.W. Van Liew, R.L. Bingner, R.D. Harmel, and T.L. Veith, 2007. Model Evaluation Guidelines for Systematic Quantification of Accuracy in Watershed Simulations. Soil & Water Division of American Society of Agricultural and Biological Engineers, 50(3): 885-900.

Nash, J.E. and J.V. Sutcliffe, 1970. River Flow Forecasting through Conceptual Models Part I—A Discussion of Principles. Journal of hydrology, 10(3): 282-290.

Nietsch, S.L., J.G. Arnold, J.R. Kiniry, and J.R. Williams, 2005. Soil and Water Assessment Tool Theoretical Documentation. Version 2005. Texas Water Resource Institute, College Station, Texas.

Priestley, C. and R. Taylor (1972). "On the assessment of surface heat flux and evaporation using large-scale parameters." Journal of American Meteroloigacal Society, vol.100, no.2, pp.81-92.

Raghavan, S. V., V. M. Tue and L. Shie-Yui (2014). "Impact of climate change on future stream flow in the Dakbla river basin." Journal of Hydroinformatics, vol.16, no.1, pp. 231-244.

Rijsberman, F. R. (2006). "Water scarcity: Fact or fiction?" Agricultural water management 80(1): 5-22.

UN-ESCWA and BGR (United Nations Economic and Social Commission for Western Asia; Bundesanstalt fürGeowissenschaften und Rohstoffe), 2013. Inventory of Shared Water Resources in Western Asia. Beirut.

Zang, C., J. Liu, M. Velde and F. Kraxner 2012. "Assessment of spatial and temporal patterns of green and blue water flows under natural conditions in inland river basins in Northwest China." Hydrology and Earth System Sciences **16**(8): 2859-2870.

ADDRESS FOR CORRESPONDENCE

Nadhir A. Al-Ansari
Department of Civil, Environmental and Natural Resources Engineering
Lulea University of Technology
Lulea, Sweden

Email: nadhir.alansari@ltu.se